National Park Service
U.S. Department of the Interior

Natural Resource Stewardship and Science

Topographic and Hydrologic Insight for the Westside Road Problem

Mount Rainier National Park

Natural Resource Report NPS/MORA/NRR—2015/1057

ON THIS PAGE
Photograph of en echelon, current-aligned logs within a channel in the Tahoma Creek valley.
Photograph courtesy of Matthew A. Thomas.

ON THE COVER
Photograph of Tahoma Creek among impacted stands of old growth forest at Mount Rainier National Park.
Photograph courtesy of Matthew A. Thomas

Topographic and Hydrologic Insight for the Westside Road Problem

Mount Rainier National Park

Natural Resource Report NPS/MORA/NRR—2015/1057

Matthew A. Thomas [1,2] , Paul Kennard[1]

[1]National Park Service
Mount Rainier National Park
55210 238th Avenue East
Ashford, WA 98304-9751

[2]now at Sandia National Laboratories
Carlsbad Field Office
4100 National Parks Highway, Building A
Carlsbad, NM 88220

October 2015

U.S. Department of the Interior
National Park Service
Natural Resource Stewardship and Science
Fort Collins, Colorado

The National Park Service, Natural Resource Stewardship and Science office in Fort Collins, Colorado, publishes a range of reports that address natural resource topics. These reports are of interest and applicability to a broad audience in the National Park Service and others in natural resource management, including scientists, conservation and environmental constituencies, and the public.

The Natural Resource Report Series is used to disseminate comprehensive information and analysis about natural resources and related topics concerning lands managed by the National Park Service. The series supports the advancement of science, informed decision-making, and the achievement of the National Park Service mission. The series also provides a forum for presenting more lengthy results that may not be accepted by publications with page limitations.

All manuscripts in the series receive the appropriate level of peer review to ensure that the information is scientifically credible, technically accurate, appropriately written for the intended audience, and designed and published in a professional manner.

This report received formal peer review by subject-matter experts who were not directly involved in the collection, analysis, or reporting of the data, and whose background and expertise put them on par technically and scientifically with the authors of the information.

Views, statements, findings, conclusions, recommendations, and data in this report do not necessarily reflect views and policies of the National Park Service, U.S. Department of the Interior. Mention of trade names or commercial products does not constitute endorsement or recommendation for use by the U.S. Government.

This report is available in digital format from the Natural Resource Publications Management website (http://www.nature.nps.gov/publications/nrpm/). To receive this report in a format optimized for screen readers, please email irma@nps.gov.

Please cite this publication as:

Thomas, M. A. and P. Kennard. 2015. Topographic and hydrologic insight for the Westside Road problem: Mount Rainier National Park. Natural Resource Report NPS/MORA/NRR—2015/1057. National Park Service, Fort Collins, Colorado.

NPS 105/30057, October 2015

Contents

Figures

Appendices

Abstract

The braided fluvial systems that flank Mount Rainier in Washington State facilitate landscape change that is appreciable on the human timescale. In Mount Rainier National Park, the debris flows and floods transmitted by these hydrogeomorphic systems have routinely challenged visitor safety, infrastructure, and the preservation of natural / cultural resources. This study focuses on the intersection of the Tahoma Creek valley and an approximately 1.5 km section of the Westside Road in the southwestern corner of the Park. Average cross-valley slopes, a relative elevation map, and one-dimensional free surface flow simulations are employed to quantitatively identify challenges associated with maintaining the problematic road section. Eighty-seven percent of the simple cross-valley slopes calculated favor the routing of water toward the road. An elevation relative to thalweg map, which highlights subtle changes in topography, reveals that the road bench is, on average, three meters above a proximal water course. One-dimensional free surface flow simulations characterize flooding risk as unevenly distributed along the road, an observation linked to local channel depth. Collectively, the topographic and hydrologic insight generated for this study indicates that it is unlikely the Westside Road, in its current form, will ever function as a low-maintenance route that accommodates public vehicular traffic. Importantly, the work reported here provides a starting point to consider along-road protection measures and a foundation to more rigorously simulate water and sediment transport for Tahoma Creek from a physics-based perspective.

Acknowledgments

The work reported here was supported by the Geological Society of America and the National Park Service under the GeoCorps (Technician ID #2014049) and Geoscientists-in-the-Park program, respectively. This study would not have been possible without the field efforts of E. Kavountzis, A. Klett, E. Knoth, R. Rossi, J. Russell, and T. Schwartz. The authors are grateful for the equipment, training, and data reduction provided by S. Beason. Thoughtful discussion with N. Legg, K. Loague, and C. Magirl, as well as editorial insight from S. Anderson, S. Beason, B. Ebel, and G. Smillie greatly improved this work.

Introduction

The steep mountain streams that descend Mount Rainier, Washington are highly energetic systems capable of transporting enormous, coarse sediment loads. On short timescales, debris flows within these braided fluvial systems can act as violent, destructive agents (Lancaster et al., 2012; Legg et al., 2014). On longer timescales, aggradation can reduce stream conveyance and increase flood potential (Beason, 2007; Czuba et al., 2012). Importantly, the hydrologic triggers for debris flows and aggradation may intensify at Mount Rainier National Park in the future. For example, climate change could facilitate less snow accumulation and greater peak winter stream flows (Snover et al., 2003; Hamlet et al., 2010). Glacier retreat continues to expose new sources of unconsolidated sediment for potential transport (Nylen, 2001). As a result of a November 2006 storm, which delivered 455 mm of rain within 36 hours, there is concern that the unprecedented damages sustained to Park infrastructure may be a foreshadowing of future impacts (Beason et al., 2011).

As an agency, the National Park Service, "…preserves unimpaired the natural and cultural resources of the National Park System for the enjoyment, education, and inspiration of this and future generations (NPS, 2015c)." One of the current challenges faced by scientists and managers at Mount Rainier National Park is the road problem. Specifically, large swathes of the northwestern and southwestern quadrants of the Park have been indefinitely closed to public vehicular traffic due to debris flows and

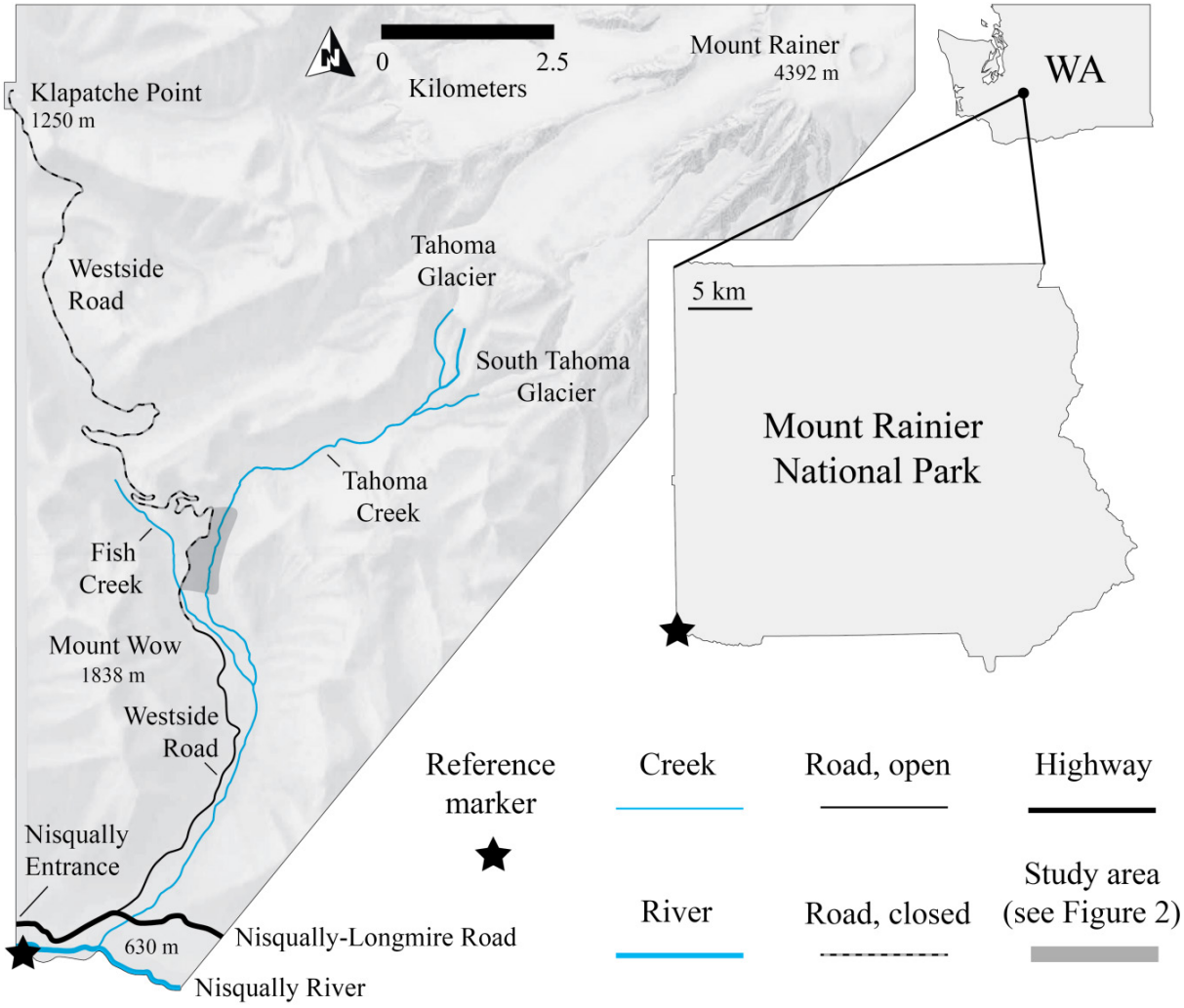

Figure 1. Location of Tahoma Creek and the Westside Road in the southwestern corner of Mount Rainier National Park, Washington (WA). Shaded topography extracted from NPS (2015a). Elevations are reported as meters above mean sea level.

flooding along the Carbon River Road and Westside Road (see Figure 1), respectively. Fortunately, there have been several efforts designed to better understand the Tahoma Creek system (see Figure 2a-b) in the vicinity of the Westside Road (e.g., NPS, 1992; Walder and Driedger, 1994; Anderson and Pitlick, 2014). The objective of this study was to employ average cross-valley slopes, a relative elevation map, and one-dimensional (1D) free surface flow simulations to quantitatively identify challenges associated with maintaining a problematic section of the road.

Study Area

The Tahoma Creek watershed is situated along the southwestern flank of Mount Rainier. As shown in Figure 1, Tahoma Creek, which is primarily sourced from the South Tahoma Glacier, with lesser contributions from the Tahoma Glacier, is a braided fluvial system that conveys water approximately 12 km before reaching the Nisqually River. During the last 41 years, at least 28 debris flows have tracked through the Tahoma Creek valley, with the most recent occurring on August 13th, 2015 (Anderson and Pitlick, 2014). Between 2002 and 2008, a period when the South Tahoma glacier retreated approximately 300 m, it is estimated that 2.3×10^6 m^3 of sediment was mobilized in the Tahoma Creek valley (Anderson and Pitlick, 2014). This study focuses upon a 1.5 km section of the Tahoma Creek valley between the Tahoma Creek trailhead and Fish Creek (see Figure 2a). The average downstream valley slope in this area is approximately four degrees. An undated deep-seated landslide deposit, just upstream of the Tahoma Creek trailhead (shown in Figure 2a), has locally reduced the valley bottom width to approximately 125 m. In the 1.5 km downstream of the landslide, the valley bottom becomes increasingly unconfined, with a width ranging up to 650 m. As shown in Figure 2a-b, the paths of extensive flooding and debris flow activity within the study area have been recorded by the destruction of old growth forest, including Red Alder (*Alnus rubra*), Western Hemlock (*Tsuga heterophylla*), and Douglas Fir (*Pseudotsuga menziesii*).

The Westside Road

The Westside Road begins at the first vehicular turnout off of the Nisqually-Longmire Road, just past the entrance gate (see Figure 1). Approximately 20 km in length, the current expression of the Westside Road ranges in elevation from approximately 650 to 1,250 m. The road, which traverses portions of the Tahoma Creek valley bottom, provides access to six major trails and at least fourteen destinations (NPS, 2015b). Designed and constructed between 1926 and

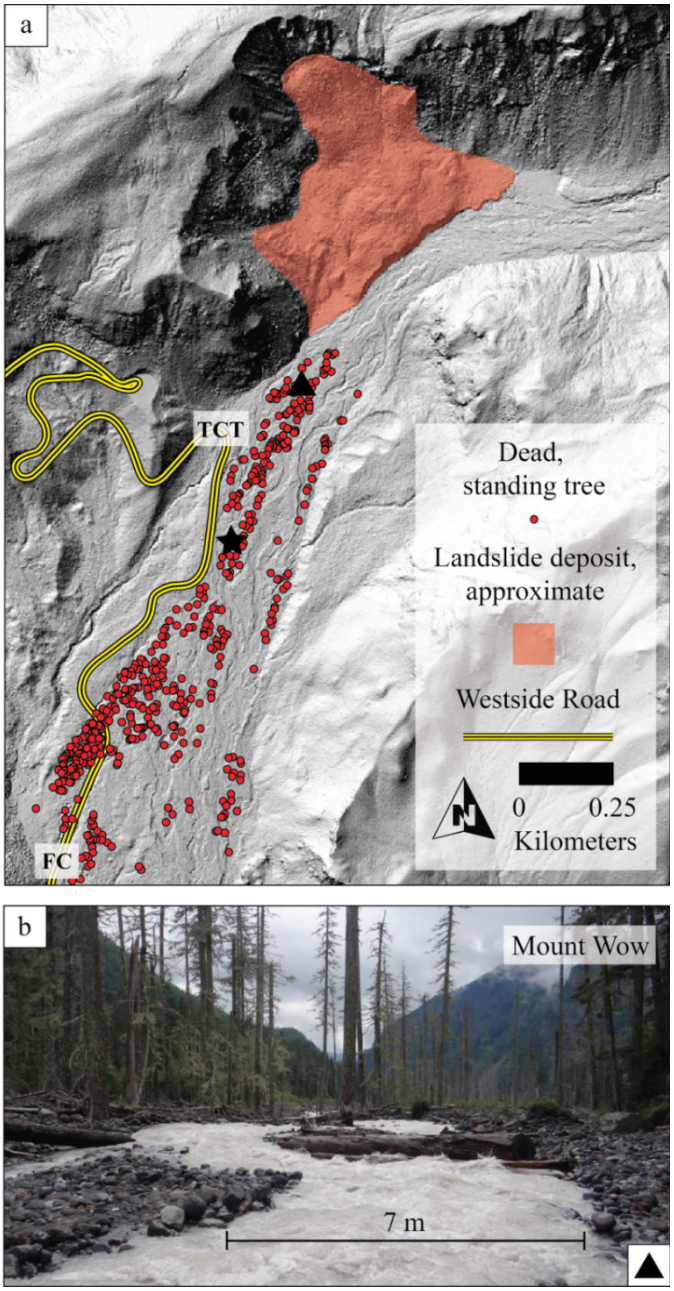

Figure 2. (a) Area focused upon for this study, spanning approximately 1.5 km from the Tahoma Creek trailhead (TCT) to Fish Creek (FC). Former location of the Tahoma Creek Campground identified with a black star. The mapped extent of dead, standing trees demonstrates that the Tahoma Creek valley bottom transitions from confined near the landslide deposit to increasingly unconfined in the downstream reach. **(b)** South-looking August 2014 photograph (location identified by black triangle in Figure 2a) of Tahoma Creek among old growth forest destroyed by flooding and / or debris flows.

1934, the Westside Road was cast as part of the Around-the-Mountain plan, an ambitious engineering project which sought to circumnavigate Mount Rainier with an aesthetically-pleasing vehicular route (Owens, 2006). The plan was never fully realized, but the evidence of its construction is split among the Mowich Lake Road (to the northwest) and the Westside Road (to the southwest). Managerial challenges associated with the Westside Road surfaced in 1967 when a series of glacial outburst floods devastated the Tahoma Creek Campground, whose former location is shown in Figure 2a (Walder and Driedger, 1994). Subsequently, floods and debris flows have damaged or destroyed Park resources (e.g., trailheads, a picnic area, and restrooms) along the route. By 1993, the Westside Road beyond Fish Creek (see Figure 1) was indefinitely closed to public vehicular traffic (Owens, 2006). The efficacy of maintaining access to vehicles in the area remains difficult and contentious.

Methods

Average Cross-Valley Slopes

Average cross-valley slopes in the study area were examined with available 2002, 2008, and 2012 aerial Light Detecting and Ranging (LiDAR) datasets (NPS, 2002; NPS, 2008; NPS 2012). The shot densities for the 2002, 2008, and 2012 LiDAR datasets in the vicinity of Tahoma Creek are approximately two, one to two, and one to four points per square meter, respectively (Anderson and Pitlick, 2014). All three LiDAR datasets were used to parameterize one meter digital elevation models. To calculate the simple gradients, an approximate valley centerline was first drafted within the ArcGIS environment. At 50 m intervals along the centerline, a perpendicular line, spanning the braided fluvial valley bottom (i.e., the cross-valley extent of discernible channels), was drawn. Next, cross-valley lines were discretized with five-meter point spacing. Elevation values were extracted from each one-meter digital elevation model for all points. Finally, a least-squares approach was used to approximate a linear trend line for each cross-valley point set, for each year. The average correlation coefficients for the three datasets range from 0.4 to 0.5. A map-view perspective of average cross-valley slopes corresponding to 2002 is shown in Figure 3 and a comparison of average cross-valley slopes for 2002, 2008, and 2012 is shown in Figure 4. Appendix A provides location information for the cross sections used for the average cross-valley slope calculations.

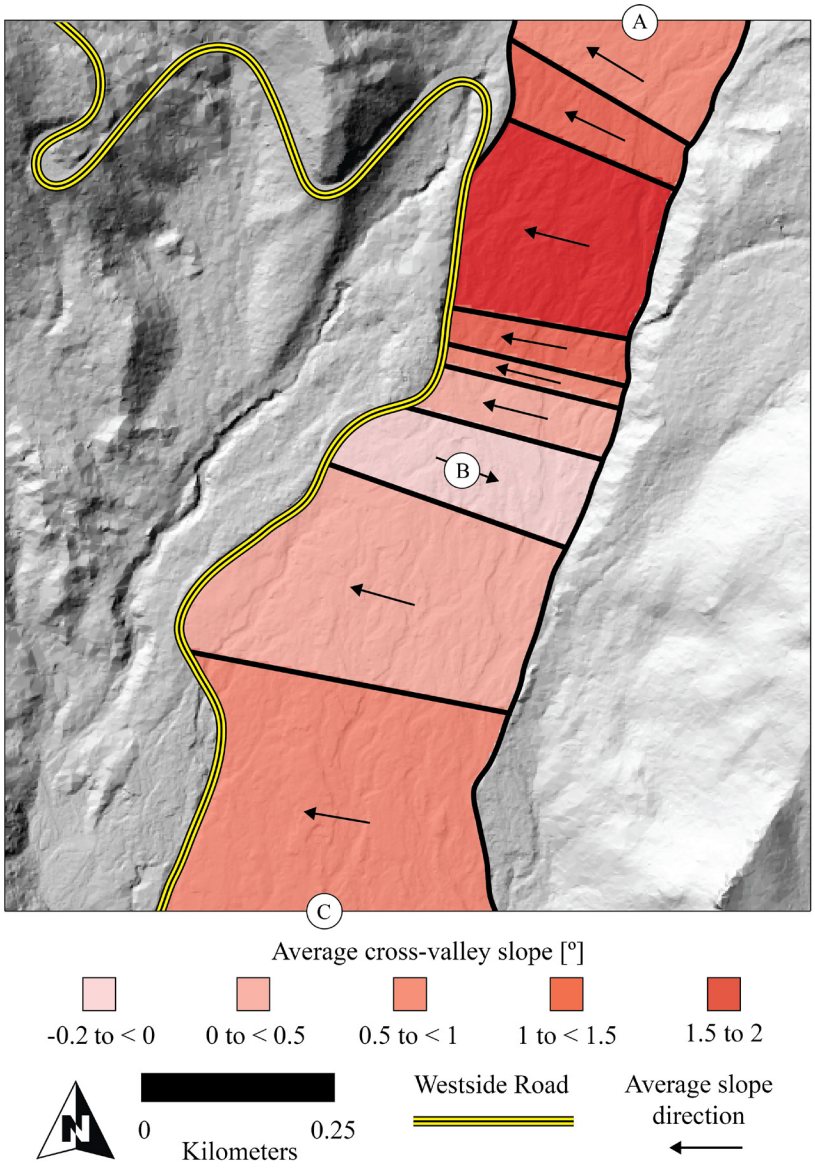

Figure 3. Average cross-valley slopes along a problematic section of the Westside Road calculated with 2002 LiDAR (NPS, 2002). Positive and negative slopes indicate westward and eastward average slope directions, respectively. The A, B, and C markers correspond approximately to the 0, 0.75, and 1.5 km downstream distances reported in Figure 4.

Landscape Elevation Relative to Thalweg

An elevation relative to thalweg (ERT) map was employed to highlight important topographic features within the study area. An ERT map provides a snapshot of topography with elevations of a landscape relative to the thalweg of interest (Jones, 2006). Obviously, there are

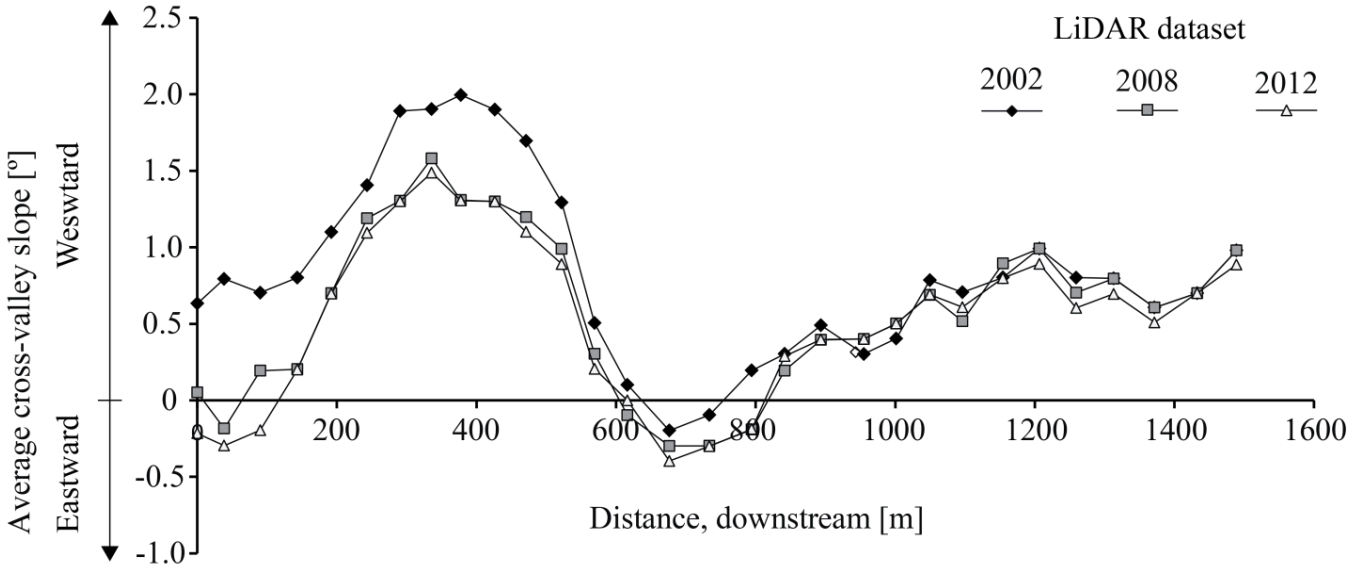

Figure 4. Comparison of average cross-valley slopes calculated with 2002, 2008, and 2012 LiDAR (NPS, 2002; NPS, 2008; NPS, 2012). The downstream (i.e., southern) distance corresponds to the centerline path for the valley area shaded in Figure 3.

many channels that comprise the Tahoma Creek system, all of which experience deposition and / or erosion over short time scales. This study focuses on a single thalweg, visible in 2002 LiDAR, as an example of a channel geometry near the road linked to historical damages along the bench. Although beyond the scope of this study, future efforts focused on developing more detailed ERT maps within the study area could sample a greater number of channels for all available LiDAR datasets.

To construct the ERT map, the channel thalweg (see Figure 5) was first identified and digitally registered with the ArcGIS Fill, Flow Direction, and Flow Accumulation tools. Next, the map-view thalweg was discretized with 50 m spacing. Elevation values corresponding to the thalweg were then extracted from the digital elevation model and assigned to its corresponding point. For each point, a line, perpendicular to the thalweg and valley centerline, was constructed, spanning the area of interest. Each line was assigned the elevation value of the single point it intersected. The thalweg elevation lines were then used to interpolate a triangular irregular network which was converted into a digital elevation model raster. Finally, the thalweg raster was subtracted from the original digital elevation model raster. The resulting ERT map, shown in Figure 5, provides a snapshot of elevations relative to the channel of interest. Appendix B provides location information for the cross sections used for the ERT calculations.

One-Dimensional Free Surface Flow Simulations

To expand upon the topographic-based insight developed for this study, 1D free surface flow simulations were employed. The channel identified for the ERT calculations was focused on for the simulation effort. The 1D water surface solutions are steady-state snapshots that do not include consideration of sediment transport. Importantly, the simulations conducted for this study were not designed to represent actual / modern-day conditions or serve as a predictive tool. The aim of these simulations was to examine the potential for flooding in a channel that was proximal to Westside Road in the study area from a bimodal (i.e., yes or no) perspective. The authors assume that water overtopping the banks of the channel inherently poses a risk to the road bench. Future efforts to estimate specific flooding depths along the road will require more sophisticated simulations that can account for multi-dimensional effects of surface flow.

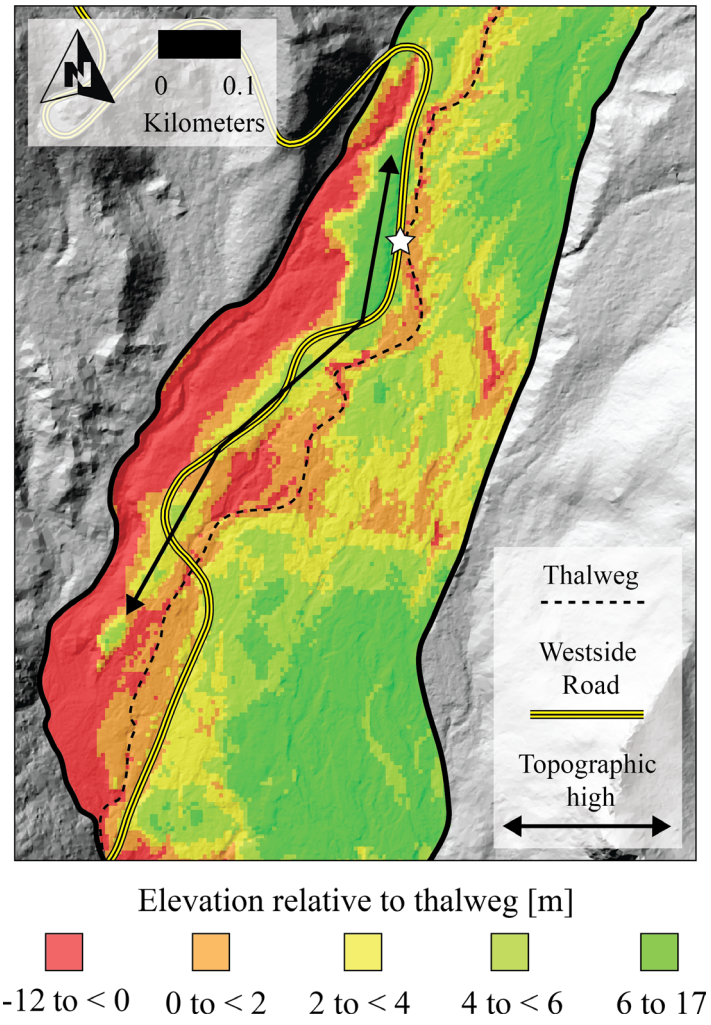

Figure 5. Elevation relative to thalweg values calculated with a water course (shown with black dash) that is discernible with 2002 LiDAR (NPS, 2002). The white star corresponds to a location where the Westside Road was inundated and eroded during a November 2006 storm.

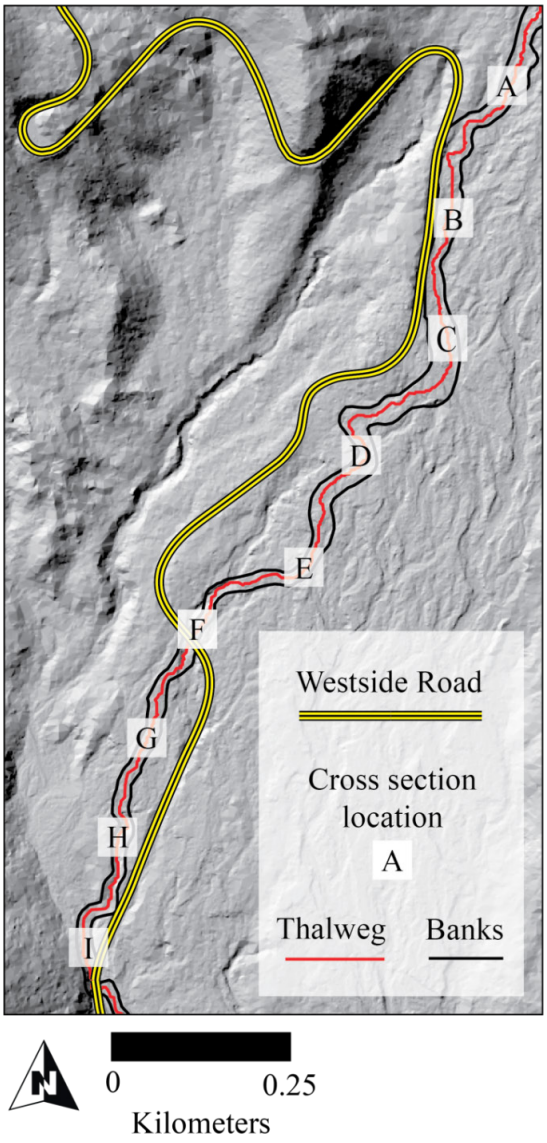

Figure 6. Cross section locations focused upon for one-dimensional free surface flow modeling. The cross section identifiers correspond to Figure 7.

The Hydrologic Engineering Center, River Analysis Systems model (HEC-RAS; USACE, 2010) and ArcGIS extension, HEC-GeoRAS (USACE, 2009), were employed to parameterize and iteratively solve the 1D energy equation (see Magirl et al., 2008):

$$y_i + z_i + \frac{\alpha_i v_i^2}{2g} = y_{i+1} + z_{i+1} + \frac{\alpha_{i+1} v_{i+1}^2}{2g} + h_e \qquad (1)$$

where i is a cross section index [-], i+1 is the next upstream cross section [-], y is the depth of water [L], z is channel invert elevation [L], α is the velocity weighting coefficient [-], v is the average velocity [LT^{-1}], g is the acceleration due to gravity [LT^{-2}], and h_e is the head energy loss [L]. The channel banks, thalweg, and cross section locations, identified in Figure 6, were drafted from available LiDAR (NPS, 2002) and registered within the HEC-GeoRAS environment. A normal depth, approximated with an average thalweg slope of 0.05 [-], was assigned as the downstream boundary condition. To minimize the impact of the boundary condition on the solution within the area of interest, the simulated reach was extended 1.5 km (i.e., twice the study area length) downstream of Fish Creek. Subcritical flow conditions were assumed throughout. A Manning's

roughness coefficient of 0.11 $s^1m^{-1/3}$ was assigned to each cross section (Jarrett, 1985). Flow rates of 12 m^3s^{-1} (i.e., Q1), 35 m^3s^{-1} (i.e., Q2), and 200 m^3s^{-1} (i.e., Q3) were used to solve for steady-state snapshots of the water surface. Q1 is an observation-based value for Tahoma Creek, near the area shown in Figure 2b, estimated by the authors in the summer of 2014. Q2 is an observation-based value recorded by the Longmire gage on the Nisqually River in the fall of 2009 (value extracted from Anderson and Pitlick, 2014), and is taken here as a reasonable surrogate for Tahoma Creek. Q3 is a literature-based outburst flow value for Tahoma Creek estimated by Walder and Driedger (1994). The flow rates selected for this study are conservative (i.e., err on the high end). Correspondingly, the results shown in Figure 7 are most useful in demonstrating how the potential for flooding could change with factor versus order of magnitude-based differences among flow rates. Appendix C provides location information for the cross sections used for the free surface flow calculations.

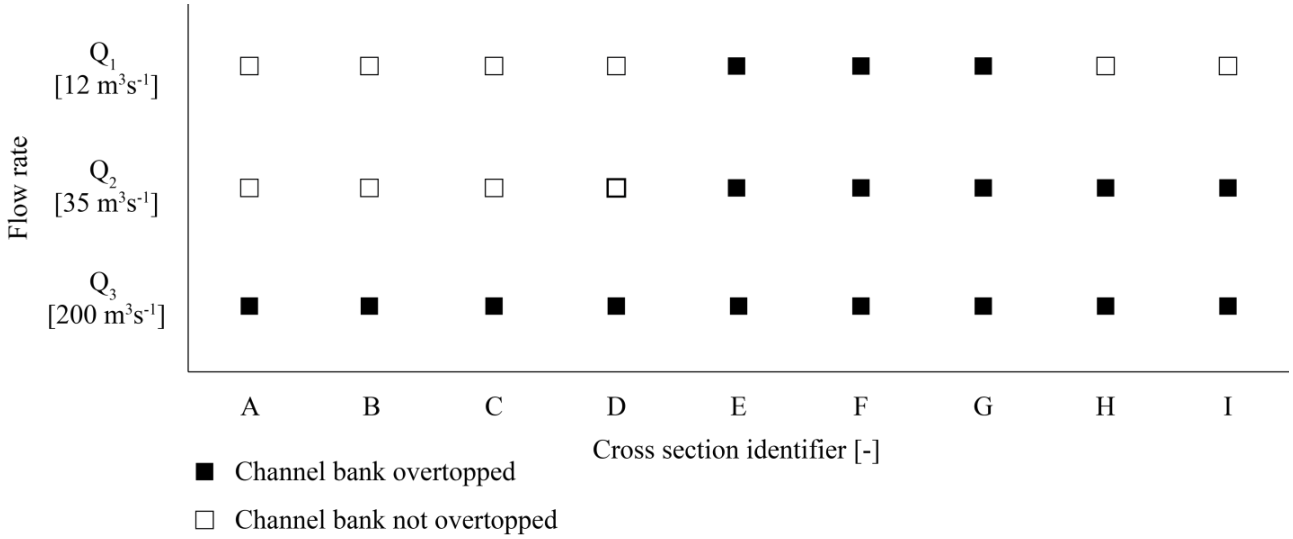

Figure 7. Positive or negative flooding response reported for cross sections A through I (see Figure 6) for the simulated Q1, Q2, and Q3 flow conditions.

Results

Average Cross-Valley Slopes

The average cross-valley slopes calculated along the study area range from zero to two degrees. Changes in average cross-valley slope are non-uniform in time. Figure 4 shows that within approximately the first 800 m of downstream distance considered, average cross-valley slopes in 2002 change by up to 1.1° by 2008 or 2012. In the remaining 700 m of downstream distance, the average cross-valley slopes only change by up to 0.2°. The transition from dynamic to relatively static average cross-valley slopes seen in Figure 4 could be related to fluvially-transported debris flow deposits within the study area. The most striking insight from the average cross-valley slopes is the precarious location of the Westside Road. As shown in Figure 4, 87 % of the cross-valley slopes calculated would, on average, convey water toward the road.

Landscape Elevation Relative to Thalweg

Although ERT calculations cannot provide insight that is physics-based, they are useful for identifying topographic features within the Tahoma Creek valley. Importantly, the ERT data in Figure 5 highlights a northeast-southwest trending topographic high that is proximal to the road. As the Westside Road departs the western-most flank of the valley adjacent to the slopes of Mount Wow (see Figure 1), the route heads northeast for about a half kilometer, dropping into the Tahoma Creek floodplain. For a short distance, the road shifts northwest, but then abruptly turns back to the northeast, climbing onto the local topographic high. For approximately another half kilometer, the road straddles the topographic high before turning north, mostly skirting the higher elevations until it meets the Tahoma Creek trailhead.

In the vicinity of the road, the average ERT value is three meters above thalweg. Although depth-frequency information is not available for the channel selected for this ERT map, it is worth noting that the flood stage associated with the November 2006 storm reached the Westside Road bench (see area labeled in Figure 5 with a star), suggesting a minimum flow depth of approximately two meters.

One-Dimensional Free Surface Flow Simulations

The simulations reported here are preliminary in that they consider a single channel under a limited number of flow conditions. Expectedly, increased flow rates lead to increased flood occurrence. For example, flooding occurs for 33, 56, and 100 % of the cross sections for the Q_1, Q_2, and Q_3 flow conditions, respectively (see Figure 7). The spatially-variable signatures of flood occurrence along the targeted channel are most useful in that they demonstrate flooding risk is unevenly distributed in the study area. These simulations can be used to broadly organize flooding risk into three categories: (1) higher, (2) intermediate, and (3) lower. Areas of higher risk include cross sections E, F, and G, with flooding under all (i.e., Q_1, Q_2, and Q_3) flow conditions. The average stage needed to cause flooding here is approximately one meter. Areas of intermediate risk include cross sections H and I, with flooding for the two largest (i.e., Q_2 and Q_3) flow conditions. The average stage needed to cause flooding here is approximately 1.5 meters. Areas of lower risk include cross sections A, B, C, and D which experience flooding only for the greatest (i.e., Q_3) flow condition. The average stage needed to cause flooding here is approximately 2.5 meters.

Discussion

The analyses conducted for this study quantitatively corroborate the managerial challenges associated with the study area. In the short term, these results may be useful, as a starting point, to prioritize the location and design of future protection measures. For example, the Figure 5 ERT map suggests that an approximately 5,000 m^3 fill-in-place operation would be needed to bring lower sections of Westside Road at least 2.5 m above the nearby channel thalweg to reduce inundation hazard. Areas in which the channel is immediately adjacent to the road (see Figure 6) could benefit from cribbing and / or engineered log jams to harden the road prism to erosion. Importantly, the efforts reported here demonstrate that flooding risk is unevenly distributed along the route, largely a function of local channel depth. For the portions of the road closest to the cross sections reported as most vulnerable to flooding (i.e., E, F, and G; see Figure 6), the installation of surface hardening measures (e.g., water bars or pavement) could help reduce erodibility. Clearly, an understanding of long-term conditions and possible design solutions would benefit from further geomorphic analysis of Tahoma Creek.

Beyond the consideration of protection measures, this study provides a firm foundation to more rigorously investigate hydrologic response for the Tahoma Creek system. For example, as shown in Figure 7, 1D free surface flow simulations suggest cross sections A, B, C, and D (see Figure 6) are susceptible to flooding for extreme (e.g., outburst-type) flow conditions. Bank erosion hazards can threaten the road bench well before those associated with inundation. Future efforts to assess along-road hazards would benefit from a consideration of water and sediment transport with more sophisticated physics-based models such as InHM (Heppner et al., 2006) and FaSTMECH (Nelson et al., 2003). Correspondingly, a more complete record of observation (e.g., rainfall, flow rate, stage, and sediment concentration) would be required to design more robust boundary conditions, effectively parameterize the system, and rigorously evaluate the results.

Summary and Conclusions

Mount Rainier constitutes a geomorphic environment in constant flux. These changes, often discernible on the human timescale, can be problematic when they challenge visitor safety, infrastructure, and the preservation of natural / cultural resources. The topographic- and hydrologic-based methods employed for this study quantitatively highlight the precarious location of the Westside Road between Fish Creek and the Tahoma Creek trailhead (see Figure 2a). First, in the most general sense, cross-valley slopes overwhelmingly favor the routing water toward the road (see Figure 4). Second, scrutiny of along-road topography with a relative elevation map demonstrates that, on average, the route is only marginally higher than a nearby channel thalweg (see Figure 5). Third, physics-based free surface flow simulations indicate that a nearby channel (see Figure 6) can flood under observation- and literature-based flow conditions (see Figure 7). Taken together, this work suggests that it is unlikely the present alignment of the road between Fish Creek and the Westside Road trailhead will ever be a low-maintenance route that serves vehicular traffic. Moving forward, the consideration of future along-road protection measures (e.g., engineered log jams, cribbing, water bars, and pavement) would benefit from a multidimensional consideration of water and sediment transport from an event-based perspective.

Literature Cited

Anderson, S. and J. Pitlick. 2014. Using repeat LiDAR to estimate sediment transport in a steep stream. Journal of Geophysical Research: Earth Surface, 119(3): 621-643.

Beason, S.R. 2007. The environmental implications of aggradation in major braided rivers at Mount Rainier National Park, Washington. Thesis. University of Northern Iowa, Cedar Falls, Iowa.

Beason, S.R., P.M. Kennard, T.B. Abbe, and L.C. Walkup. 2011. Landscape response to climate change and its role in infrastructure protection and management at Mount Rainier National Park. Park Science, 28(2): 31-55.

Czuba, J.A., C.S. Magirl, C.R. Czuba, C.A. Curran, K.H. Johnson, T.D. Olsen, H.K. Kimball, and C.C. Gish. 2012. Geomorphic analysis of the river response to sedimentation downstream of Mount Rainier, Washington. United States Geological Survey, Reston, Virginia. Open File Report 2012-1242.

Hamlet, A.F., P. Carrasco, J. Deems, M.M. Elsner, T. Kamstra, C. Lee, S.-Y. Lee, G.S. Mauger, E.P. Salathe, I. Tohver, and L.W. Binder. 2010. Final project report for the Columbia Basin climate change scenarios project. Accessed 13 April 2015 at http://warm.atmos.washington.edu/2860/report/.

Heppner, C.S., Q. Ran, J.E. VanderKwaak, and K. Loague. 2006. Adding sediment transport to the integrated hydrology model (InHM): Development and testing. Advances in Water Resources, 29(6): 930-943.

Jarrett, R.D. 1985. Determination of roughness coefficients for streams in Colorado. United States Geological Survey, Lakewood, Colorado. Water-Resources Investigations Report 85-4004.

Jones, J.L. 2006. Side channel mapping and fish habitat suitability analysis using LiDAR topography and orthophotography. Photogrammetric Engineering and Remote Sensing, 71(11): 1202-1206.

Lancaster, S.T., A.W. Nolin, E.A. Copeland, and G.E. Grant. 2012. Periglacial debris-flow initiation and susceptibility and glacier recessions from imagery, airborne LiDAR, and ground-based mapping. Geosphere, 8(2): 417-430.

Legg, N.T., A.J. Meigs, G.E. Grant, and P.M. Kennard. 2014. Debris flow imitation in proglacial gullies on Mount Rainier, Washington. Geomorphology, 226: 249-260.

Magirl, C.S., M.J. Breedlove, R.H. Webb, and P.G. Griffiths. 2008. Modeling water-surface elevations and virtual shorelines for the Colorado River in Grand Canyon, Arizona. United States Geological Survey, Reston, Virginia. Scientific Investigations Report 2008-5075.

National Park Service (NPS). 1992. Environmental assessment for management of the Westside Road, Mount Rainier National Park, Washington. Ashford, Washington.

National Park Service (NPS). 2002. Tahoma Creek LiDAR survey. National Park Service unpublished data, Ashford, Washington.

National Park Service (NPS). 2008. Park-wide LiDAR survey. National Park Service unpublished data, Ashford, Washington.

National Park Service (NPS). 2012. Tahoma Creek LiDAR survey. National Park Service unpublished data, Ashford, Washington.

National Park Service (NPS). 2015a. Mount Rainier Plan Your Visit Park-wide Map website. Available at: http://www.nps.gov/mora/planyourvisit/index.htm/ (accessed 14 April 2015).

National Park Service (NPS). 2015b. Trails of Mount Rainier website. Available at: http://www.nps.gov/mora/planyourvisit/trails-of-mount-rainier.htm/ (accessed 13 April 2015).

National Park Service (NPS). 2015c. What We Do website. Available at: http://www.nps.gov/aboutus/index.htm/ (accessed 20 April 2015).

Nelson, J.M., J.P Bennett, and S.M. Wiele, 2003, Flow and sediment transport modeling in M. Kondolph and H. Piegay, editors. Tools in Geomorphology. Wiley and Sons, Chichester, United Kingdom.

Nylen, T.H. 2001. Spatial and temporal variations of glaciers (1913-1994) on Mt. Rainier and relation with climate. Thesis. Portland State University, Portland, Oregon.

Owens, E. 2006. National Park Service Cultural Landscape Inventory 2006 Westside Road Mount Rainier National Park. National Park Service, Seattle, Washington.

Snover, A.K., A.F. Hamlet, and D.P. Lettenmaier. 2003. Climate change scenarios for water planning studies: pilot applications in the Pacific Northwest. Bulletin of American Meteorological Society 84(11): 1513-1518.

United States Army Corps of Engineers (USACE). 2009. HEC-GeoRAS GIS tools for support of HEC-RAS using ArcGIS. United States Army Corps of Engineers, Davis, California.

United States Army Corps of Engineers (USACE). 2010. HEC-RAS River Analysis System User's Manual 4.1. United States Army Corps of Engineers, Davis, California.

Walder, J.S. and Driedger, C.L. 1994. Geomorphic change caused by outburst floods and debris flows at Mount Rainier, Washington, with emphasis on Tahoma Creek valley. United States Geological Survey, Vancouver, Washington. Water-Resources Investigations Report 93-4093.

Appendix A: Average Cross-Valley Slopes

Table A-1. Location information for cross sections used for average cross-valley slope calculations.

Cross section	Start point[1]		End point[1]	
	Easting	Northing	Easting	Northing
CVS-1	585559.3	5183164.3	585711.9	5183033.0
CVS-2	585524.4	5183130.5	585692.4	5182993.1
CVS-3	585476.9	5183100.0	585667.8	5182950.7
CVS-4	585428.5	5183060.7	585654.2	5182904.9
CVS-5	585403.1	5183007.8	585630.4	5182875.2
CVS-6	585412.4	5182935.4	585623.7	5182837.0
CVS-7	585386.9	5182878.5	585609.2	5182810.0
CVS-8	585349.0	5182836.7	585597.9	5182772.0
CVS-9	585342.5	5182792.2	585587.4	5182734.8
CVS-10	585337.7	5182738.1	585580.9	5182691.2
CVS-11	585330.9	5182695.1	585558.4	5182649.1
CVS-12	585324.7	5182645.9	585554.4	5182596.2
CVS-13	585319.1	5182602.3	585547.8	5182545.9
CVS-14	585292.5	5182561.8	585533.2	5182499.6
CVS-15	585216.4	5182537.5	585509.4	5182448.0
CVS-16	585178.0	5182497.5	585488.2	5182389.8
CVS-17	585157.0	5182443.3	585461.8	5182342.2
CVS-18	585109.9	5182401.7	585448.6	5182303.9
CVS-19	585054.3	5182363.4	585440.6	5182261.5
CVS-20	585005.4	5182314.4	585423.4	5182217.9
CVS-21	584986.9	5182268.1	585406.7	5182178.0
CVS-22	585018.6	5182203.3	585397.1	5182141.3
CVS-23	585046.4	5182151.7	585382.7	5182102.3
CVS-24	585036.6	5182084.5	585359.0	5182063.2
CVS-25	585013.7	5182031.9	585370.8	5182012.3
CVS-26	584991.6	5181978.4	585377.1	5181961.2
CVS-27	584968.3	5181917.6	585386.4	5181916.2
CVS-28	584944.9	5181859.6	585399.6	5181858.0
CVS-29	584919.5	5181797.7	585408.2	5181797.7
CVS-30	584900.8	5181737.5	585379.3	5181737.5

[1]Coordinates referenced in UTM NAD83 Zone 1, Meters

Appendix B: Landscape Elevation Relative to Thalweg

Table B-1. Location information for cross sections used for elevation relative to thalweg calculations.

Cross section	Start point[1]		Thalweg[1]		End point[1]	
	Easting	Northing	Easting	Northing	Easting	Northing
ERT-1	585570.8	5183199.2	585592.7	5183182.5	585745.7	5183066.3
ERT-2	585554.1	5183161.1	585569.6	5183148.3	585713.6	5183029.3
ERT-3	585517.5	5183134.8	585558.8	5183099.4	585689.3	5182987.7
ERT-4	585468.7	5183106.4	585514.9	5183070.5	585669.1	5182950.6
ERT-5	585408.7	5183069.8	585483.2	5183020.2	585654.8	5182906.0
ERT-6	585354.7	5183033.3	585461.6	5182972.1	585628.7	5182876.5
ERT-7	585327.0	5182977.9	585443.7	5182922.3	585621.1	5182837.8
ERT-8	585308.0	5182927.1	585418.5	5182883.9	585607.6	5182810.0
ERT-9	585286.8	5182878.4	585384.1	5182845.4	585600.1	5182772.1
ERT-10	585248.7	5182829.8	585368.0	5182795.4	585591.6	5182730.8
ERT-11	585219.1	5182781.1	585360.5	5182744.8	585582.4	5182687.8
ERT-12	585191.6	5182734.5	585347.9	5182698.2	585570.6	5182646.6
ERT-13	585168.3	5182692.2	585346.4	5182647.1	585558.0	5182593.5
ERT-14	585153.5	5182647.7	585362.4	5182593.7	585546.2	5182546.3
ERT-15	585130.9	5182610.8	585360.6	5182546.3	585534.4	5182497.5
ERT-16	585082.3	5182583.2	585305.3	5182510.8	585512.5	5182443.6
ERT-17	585035.9	5182547.1	585233.1	5182479.9	585490.6	5182392.2
ERT-18	584996.0	5182497.7	585239.9	5182417.1	585470.4	5182340.8
ERT-19	584966.0	5182444.0	585194.9	5182377.8	585459.4	5182301.3
ERT-20	584939.8	5182392.8	585193.1	5182326.0	585443.4	5182260.0
ERT-21	584912.3	5182336.5	585168.1	5182278.1	585432.5	5182217.9
ERT-22	584883.1	5182290.7	585057.9	5182253.2	585411.4	5182177.4
ERT-23	584856.4	5182240.7	585036.3	5182207.0	585388.5	5182141.2
ERT-24	584823.9	5182184.0	585010.6	5182155.9	585382.8	5182100.0
ERT-25	584805.5	5182113.6	584980.6	5182097.7	585365.1	5182062.9
ERT-26	584799.2	5182042.4	584957.2	5182034.3	585368.5	5182013.2
ERT-27	584798.6	5181983.1	584933.9	5181978.1	585382.8	5181961.8
ERT-28	584813.6	5181919.4	584928.4	5181919.0	585396.4	5181917.4
ERT-29	584833.0	5181861.3	584921.1	5181860.8	585408.9	5181858.2
ERT-30	584874.2	5181798.2	584885.0	5181798.2	585410.6	5181798.2
ERT-31	584889.8	5181737.6	584895.9	5181737.7	585379.8	5181739.0
ERT-32	584894.4	5181679.4	584946.1	5181679.2	585373.1	5181678.2

[1]Coordinates referenced in UTM NAD83 Zone 1, Meters

Appendix C: One-Dimensional Free Surface Flow Simulations

Table C-1. Location information for cross sections used for free surface flow calculations.

Cross section	Left overbank[1]		Thalweg[1]		Right overbank[1]	
	Easting	Northing	Easting	Northing	Easting	Northing
FSF-A	585569.8	5183166.2	585574.7	5183164.4	585583.8	5183161.1
FSF-B	585477.2	5183052.6	585493.9	5183045.5	585507.4	5183040.1
FSF-C	585430.6	5182923.5	585442.3	5182918.5	585462.9	5182909.4
FSF-D	585345.9	5182748.1	585360.4	5182746.7	585378.6	5182745.0
FSF-E	585353.1	5182591.7	585362.3	5182591.7	585378.6	5182591.3
FSF-F	585245.4	5182440.5	585256.1	5182436.3	585268.8	5182431.5
FSF-G	585166.8	5182289.7	585174.5	5182286.4	585180.6	5182283.6
FSF-H	585015.0	5182197.9	585025.0	5182193.1	585035.2	5182188.4
FSF-I	584959.0	5182063.2	584968.0	5182059.2	584972.4	5182057.1
FSF-J	584914.0	5181939.1	584930.2	5181930.8	584950.0	5181921.1
FSF-K	584885.9	5181783.7	584892.6	5181783.1	584899.3	5181782.4
FSF-L	584973.5	5181656.2	584982.5	5181657.9	584992.1	5181659.4
FSF-M	585040.1	5181484.3	585047.9	5181488.0	585060.2	5181494.3
FSF-N	585127.2	5181365.8	585135.2	5181370.5	585143.5	5181375.5
FSF-O	585333.0	5181214.8	585345.6	5181229.0	585366.9	5181252.0
FSF-P	585480.8	5181047.8	585501.1	5181068.6	585509.3	5181077.4
FSF-Q	585641.8	5180932.8	585648.4	5180937.2	585666.5	5180945.4
FSF-R	585638.5	5180752.7	585652.2	5180753.2	585672.5	5180753.8
FSF-S	585632.8	5180541.3	585646.3	5180541.5	585676.1	5180542.5

[1]Coordinates referenced in UTM NAD83 Zone 1, Meters

The Department of the Interior protects and manages the nation's natural resources and cultural heritage; provides scientific and other information about those resources; and honors its special responsibilities to American Indians, Alaska Natives, and affiliated Island Communities.

NPS 105/30057, October 2015

National Park Service
U.S. Department of the Interior

Natural Resource Stewardship and Science
1201 Oak Ridge Drive, Suite 150
Fort Collins, Colorado 80525

www.nature.nps.gov